Pak. J. Bot., 52(6): 2165-2174, 2020. DOI: http://dx.doi.org/10.30848/PJB2020-6(36)

IDENTIFICATION AND MAPPING OF AN EARLY LEAF SENESCENCE TRAIT, *es2* MUTANT, IN RICE

SITTIPUN SINUMPORN[1,2], YUYU CHEN[1,2], PEIPEI ZHANG[1,2], YINGXIN ZHANG[1,2], LIAQAT SHAH, YONGRUN CAO[1,2], NING YU[1,2], PING YU[1,2], WEIXUN WU[1,2], , LIYONG CAO[1,2,3] AND QUNEN LIU[1,2*]

[1]Key Laboratory for Zhejiang Super Rice Research, China National Rice Research Institute, Hangzhou, Zhejiang, 310006, China
[2]State Key Laboratory of Rice Biology, China National Rice Research Institute, Hangzhou, Zhejiang 310006, China
[3]Collaborative Innovation Center of Henan Grain Crops, Henan Agricultural University, Zhengzhou, Henan, 450002, China
[*]Corresponding author's email: liuqunen202@163.com; Tel: 86-571-63370265; Fax: 86-571-63370265

Abstract

Leaf senescence is the final stage of leaf development. Early senescence has negative impacts on crop productivity, especially in rice. In this study, *early leaf senescence on chromosome 2 mutant*, designated as *es2*, was generated by ethyl methanesulfonate (EMS) mutagenesis. Senescence symptom in *es2* appeared at the late tillering stage, and was coincidence with elevated level of cell death, sugar content, and facilitated by senescence-associated genes (SAGs) transcription. Further, oxidative stress such as hydrogen peroxide (H_2O_2), oxidative stress byproducts such as malondialdehyde (MDA), and reactive oxygen species (ROS) contents were elevated in *es2* while soluble protein content was decreased. Chloroplast ultrastructure of *es2* was filled with larger in size of starch granule and higher in number of osmophilic plastoglobuli, along with looser thylakoid symptom. At the heading stage, *es2* exhibited sharply decreasing of net photosynthetic rate (NPR) beginning from 14-28 days after heading. Consistently, *es2* photosynthetic rate was dramatically lower than wild type (WT) in flag leaf, the second leaf from top, and the third leaf from top. Using map-based cloning technique, we identified that the target gene was anchored between RM12538 and RM12729 on the short arm of chromosome 2. Finally, this research provides a novel early leaf senescence mutant characterization in rice.

Key words: *Oryza sativa*, Early leaf senescence mutant, SAGs, Reactive oxygen species (ROS), Mapping.

Introduction

Leaf is special organ with an autotrophic property. It is known as the major source for world's energy through its capacity for photosynthesis (Woo *et al.*, 2013). Leaf senescence is an age-dependent behavior and in cooperation with internal and external factors. The process is associated with cellular and organism death (Lim *et al.*, 2007). The cell death at local spot induces senescence onset and further expands throughout leaf area. Typically, loss of chlorophyll initiates at leaf border and subsequently develops into the internal leaf area. Dismantle of macromolecule such as lipids, proteins, and nucleic acids occur shortly after chlorophyll degradation period and follow by recycle of nutrients to reproductive tissue or emerging organ (Quirino *et al.*, 2000; Lim *et al.*, 2007). Elevating of sugar content along with decreasing of net photosynthetic rate (NPR) initiate leaf senescence in many cases (Nooden *et al.*, 1997; Wingler *et al.*, 1998; Quirino *et al.*, 2001; Jongebloed *et al.*, 2004; Wu *et al.*, 2013; Li *et al.*, 2014). Too early or too late senescence has negative effect to rice yield. Crop cannot maximize its full capacity for yield storage in early senescence circumstance, while nutrient remobilizing is prevented in too late senescence. Many parameters can be used to determine senescence symptom in particular mutant.

Reactive oxygen species (ROS) plays an important role in leaf senescence control (Leng *et al.*, 2017). ROS and byproducts are simultaneously accumulating throughout photosynthesis and respiration processes. Basically, ROS is slowly accumulated in plant at all growth stage but elevating prone in the presence of biotic and abiotic stresses. Senescence induces ROS accumulation, at the same time ROS caused widespread senescence. Cell and cell component could be damaged by ROS, where promotion of lipid peroxidation, degradation of membrane occurs and, consequently, elevates leaf senescence. To strike against ROS, in order to avoid cell damage, plant utilized the enzymatic mechanism such as catalase (CAT) to counteract ROS. Therefore, measurement of total antioxidant capability (T-AOC) is widespread employed for senescence marker (Navabpour *et al.*, 2003; Chakrabarty *et al.*, 2007). Malondialdehyde (MDA) is arisen as a result of fatty acid peroxidation. Further, MDA is useful biomarker to pursue oxidative stress (Del Rio *et al.*, 2005).

Many genes expressed during the mature leaf period were inhibited or down regulated at senescence stage (Gan, 2007). In *Arabidopsis*, for example, about 10% of total genes alter transcription level in senescence leaf (Guo *et al.*, 2004). Although, up to present, no any single gene was solely accredited for senescence regulatory, however, it well accepted that senescence was controlled by molecular genetic mechanism, of which regulated by various genes (Nam, 1997). Group of genes that up-regulate during leaf senescence, designated as Senescence Associated Genes (SAGs), lead to diminished many biomolecules content in leaf such as proteins, chlorophylls, carotenoids, and lipids in leaf. This is likely due to nutrient recycling process has taken place in senescence leaf (BuchananWollaston & Ainsworth, 1997; Lim *et al.*, 2007). SAGs expression level was determined to ensure that genuine leaf senescence occurred in particular mutant. To date, enormous senescence promoting genes have been studied and reported. *SGR* promotes chlorophyll degradation and is essential for chlorophyll breakdown in rice (Jiang *et al.*, 2007). *WRKY80* was up-regulated in response to ABA treatment

and dark-induced senescence (Ricachenevsky *et al.*, 2010). *OsSWEET5* regulates the galactose distribution, ectopic expression level induces sugar imbalance, leading to precocious leaf senescence (Zhou *et al.*, 2014). On the other hand, senescence interrupting genes have also been reported. *OsDOS* and *OsTZF1*, for example, play negative role to leaf senescence (Kong *et al.*, 2006; Jan *et al.*, 2013). *SUB1A* is ethylene negative mediator and hindrance senescence (Fukao *et al.*, 2012). Cell cycle and leaf senescence function is controlled by *PECTATE LYASE-LIKE* (*PLL*) (Leng *et al.*, 2017).

In the present study, we identified a mutant variant of precocious leaf senescence, *es2*, which was induced by ethyl methanesulfonate (EMS), termed *es2*. We found that senescing leaf in *es2* appeared at late tillering stage. Top three leaves of *es2* turned yellowish along with a number of senescence parameters favored to senescence characteristic. Map-based cloning suggests that *es2* possibly located on the short arm of chromosome 2. These findings provide a state-of-the-art evidence for scientific research community regarding leaf senescence in rice.

Materials and Methods

Plant materials: A premature senescence mutant line, termed *es2*, generated from rice cv. Changlijing [*Oryza sativa* L. ssp. *Japonica* cv. Changlijing, (later designated as WT)], of which was induced by exposure to 1% EMS mutagen. *es2* was crossed with the rice cv. Zhonghui 8015 [*Oryza sativa* L. ssp. *Indica* cv. Zhonghui 8015 (8015)]. F_2 population was generated for the analysis of genetic linkage and molecular mapping of *es2*. WT, *es2*, and F_2 population were grown at the experimental station of China National Rice Research Institute (CNRRI) in Hangzhou, China. DNA samples were extracted from leaves of F_2 population showing senescence phenotype using CTAB (Cetyltrimethylammonium bromide) as described by Murray & Thompson (1980). *es2* seed use in this study was M_2 generation.

Cell death and sugar content assessment: Cell death during senescence process was determined using Evans blue staining solution as previously described (Kong & Li, 2011; Li *et al.*, 2014). The second leaf from top of WT and *es2* were immersed into 10 ml of 0.25% (w/v) Evans blue solution. Leaves were then incubated for 1-2 days period and briefly washed in ddH_2O and destained by boiling in 96% ethanol solution for 10 min. The destained leaves images were captured with digital camera D800 (Nikon, Japan). Soluble sugar content was determined using anthrone reagent method as previously described (Shi *et al.*, 2016). Calculation method, based on the standard curve, was subsequently performed.

RNA extraction and quantitative RT-PCR (qRT-PCR) analysis: Total RNA were extracted from the second leaf from top at late tillering stage using RNAprep pure Kit (TIANGEN, China). cDNA was synthesized using ReverTra Ace quantitative PCR RT Master Mix Kit with gDNA remover (Toyobo, Japan). qRT-PCR reactions were conducted using SYBR Premix Ex Taq II (Takara, Japan) and then performed with Light cycler 480 System (Roche, Germany). Details of primers are listed in Table 1.

Characterization of chloroplast ultrastructure using transmission electron microscope (TEM): For TEM inspection, the top leaf from the WT and the *es2* were fixed using 2.5% glutaraldehyde in phosphate buffer (pH 7.0) for overnight at 4°C. The specimens were rinsed for three times in phosphate buffer, and then washed using 2% OsO_4 in phosphate buffer (pH 7.0) at 4°C for 1 h. The samples then washed further for three times in phosphate buffer and finally dehydrated in graded series of ethanol (30%-100%). The samples were embedded in acrylic resin, cut into ultra-thin sections, stored on uncoated nickel grids, double stained with uranyl acetate and lead citrate, and photographed using a TEM Model H-7650 (Hitachi, Japan) at Center of Electron Microscopy, Zhejiang University.

Photosynthetic rate and agronomic traits measurements: Photosynthetic rate measurement was conducted on sunny day during 9:00-12:00 a.m. every 7 days for 5 weeks starting at the beginning of the heading date using portable Li-6400XT (LICOR, USA) machine. The light intensity of measurement was set to be 1,200 µmol m^{-2} s^{-1}. For agronomic traits, 1,000-grain weight, grain size, number of grains per panicle, panicle length, and seed setting rate of the WT and *es2* were recorded.

Hydrogen peroxide (H_2O_2) and superoxide accumulation assessment: H_2O_2 accumulation was detected as described previously (ThordalChristensen *et al.*, 1997). The second leaf from top of WT and *es2* were detached and immersed into 1mg/ml of 3, 3'-Diaminobenzidine (DAB) solution (pH 3.8) for 8 h under light. After that immersed leaves were boiled in 96% ethanol solution for 10 min. The destained leaves images were captured with digital D800 (Nikon, Japan). Superoxide accumulation was assessed using nitrobluetetrazolium (NBT). Leaves were immersed into NBT solution (1 mg/mL NBT, 10 mM NaN_3, 10 mM potassium phosphate buffer, pH 7.8) as described (Mao *et al.*, 2017). Leaf images were captured with digital camera D800 (Nikon, Japan).

Table 1. List of primers use for qRT-PCR.

Gene	Forward primers (5'-3')	Reverse primers (5'-3')
SGR	AGGGGTGGTACAACAAGCTG	GCTCCTTGCGGAAGATGTAG
Osl85	GAGCAACGGCGTGGAGA	GCGGCGGTAGAGGAGATG
Osh36	GCACGGAGGCGAACGA	TTGAGCGGTAGCACCCATT
RCCR1	CGCATTTCCTCATGGAATTT	CTTCTCACGCTGTTTGTCCA
OsLOX8	CGATCGACATCAGGGATCTCA	CCACATTGTGCGCGTAGCT
HEMA1	ATGGAGGCCCAAACAATCATC	GCGTAGGACCTCAGCTTCTTGA
Actin	CAGGCCGTCCTCTCTCTGTA	AAGGATAGCATGGGGGAGAG

Dark-induced senescence and chlorophyll measurements: For dark-induced senescence detached leaves were kept in dark for 5 days at 30 ºC. For chlorophyll content measurement, ~100 mg of fresh weight leaves were immersed in 10 ml of 80% acetone solution. The leaves were kept in the dark at room temperature for 16 h. and absorbance A_{645} and A_{663} were measured using spectrophotometer DU-800 (Beckman-Coulter, USA) and calculate as previously described (Kong *et al.*, 2006).

Determination oxidative stress and byproducts: For oxidative stress indicators such as the content of H_2O_2, MDA, soluble protein content, CAT, and T-AOC were assessed using the correspondence kit from Nanjing Jiancheng technology company (Nanjing, China).

Genetic mapping of *es2*: The F_2 population from the cross of *es2*/8015 was utilized for genetic mapping. SSR marker sequences were retrieved from the previous report (McCouch *et al.*, 2002) were screened for polymorphic and further used for mapping. F_2 plants exhibit early senescence were used for chromosome screening throughout the rice chromosome. Total 102 F_2 plants showed early senescence selected from the cross between *es2*/8015 were used for genetic mapping. Genotypes of individual plant in each marker were read by gel electrophoresis.

Results

***es2* exhibited early leaf senescence at the late tillering stage:** The occurrences of yellow leaf owing to chlorophyll degradation is the common symptom and obvious visual changes in senescence leaf (Guo and Gan, 2005). During the seedling stage, the WT and *es2* showed no obvious morphological difference. However, *es2* exhibited yellow leaves at the late tillering stage onward. Early senescence process was noticeable after pronounced of yellowing leaves at ~75 days after sowing (Fig. 1a). Further, three upper yellowing leaves of *es2* (flag leaves, the second leaves and the third leaves from top) were clearly observed since the late tillering stage onward (Fig. 1b). Moreover, chlorophyll content from the second leaf from top of *es2* was significantly lower than WT at ~75 days after sowing (Fig. 1c). Stress occurred during senescence caused cell death and is irreversible process (van Doorn & Woltering, 2004). To investigate the difference of cell death scenario in the WT and *es2*, the second leaf from top of WT and *es2* at ~ 75 days were used for histochemical analysis. Evans blue staining results showed that dark blue color was obviously observed in the *es2* leaves, while it was not stained the WT leaves (Fig. 1d), indicating that the higher accumulation in number of dead cells was occurred in *es2*. Previous study reported that rising of sugar and decreasing of protein content is common condition in senescence leaf (Wingler *et al.*, 1998; Lim *et al.*, 2007). In the present study, calculated percentage of soluble sugar in *es2* was higher than that of the WT (Fig. 1e), while soluble protein content in *es2* was significantly lower (Fig. 1f). These results suggested that onset of leaf senescence was occurred in *es2*.

Reactive Oxygen Species (ROS) is highly accumulated in *es2*: Increasing of H_2O_2 content induces oxidative reaction by generates nitric oxide and lead to senescence (Wang *et al.*, 2013). DAB interacts with H_2O_2 yields dark-brown color on stained leaf. We performed DAB staining as an indicator of H_2O_2 accumulation using leaves at ~75 days after sowing date from WT and *es2*. After DAB staining, dark-brown color was detected in *es2* leaves, however, pale color was appeared in the WT leaves (Fig. 2a). To determine superoxide radical accumulation, NBT histochemical staining assay was performed. The result indicated that *es2* leaves contained higher superoxide content compared to WT, as the blue color was detected in *es2* leaves but not in WT leaves (Fig. 2b). H_2O_2 accumulation caused leaf senescence and was employed as one of senescence inducing markers (Liang *et al.*, 2014). H_2O_2 content assessment in WT and *es2* showed that it was increased in *es2*, compared to WT (Fig. 2c). This H_2O_2 accumulation assessment result was in correspondence with DAB staining. Moreover, we found that MDA accumulated at higher level in *es2* (Fig. 2d) and T-AOC assessment result indicated that T-AOC was significantly higher in *es2* (Fig. 2e). Overall, ROS assessment results and its related enzyme activity implied that *es2* contained ROS parameter favored to leaf senescence. CAT transforms H_2O_2 into water and oxygen form. It is one of an important enzyme in many organisms (Chelikani *et al.*, 2004). Our study indicated that CAT activity in WT was slightly higher than *es2* (Supplemental Fig. 1).

Chlorophyll degradation is enhanced in *es2*: Since degradation of chloroplast is marker event for leaf senescence. We further investigated whether chloroplast structure of *es2* was suffered from the senescence using TEM. The leaf samples of WT and *es2* were sampling for TEM investigation. The condensed thylakoid and grana with negligible osmophilic plastoglobuli lipoprotein were observed in the WT (Fig. 3a, c, and e). On the other hand, the chloroplast structure of *es2* contained a number of chloroplast degradation symptoms compared to WT such as loosen shaped of thylakoid, altered in grana shape, larger size of starch granules accumulated in mesophyll and higher in number of plastoglobuli lipoprotein (Fig. 3b, d, and f). These results supported that chloroplasts of *es2* rapidly degraded, compare to WT.

Since darkness is the powerful tool to assess the synchronous chlorophyll degradation and usually conducted in a number of senescence-related studies (Quirino *et al.*, 2000). In order to investigate the chlorophyll degradation rate in *es2*, detached leaves from WT and *es2* were incubated under dark condition with adaxial up orientation for 5 days. The result showed that detached leaves of *es2* turned almost completely to yellowish in color while partially of detached leaves from WT turned into yellow (Fig. 4a). To determine whether chlorophyll content was different between WT and *es2* after 5 days under dark incubation, we test chlorophyll content from three samples each of WT and *es2*. The result indicated that chlorophyll content of detached leaves of *es2* were observably lower than those of WT under 5 days in dark condition (Fig. 4b). To clarify in further detail, before dark treatment, chlorophyll content ratio of WT: *es2* was

~1.46, however, chlorophyll content ratio, after dark incubation, was raised to ~18.12, indicated that chlorophyll degradation rate was accelerated in *es2* under dark incubation. We further investigated two SAGs expression level at 0, 1, and 3 days after dark-induced senescence for *Osh36* and at 0 and 1 days for *RCCR1*. *Osh36* encodes aminotransferase are only associated with dark-induced senescence (Lee *et al.*, 2001). *RCCR1* controls leaf senescence, particularly, chlorophyll degradation (Tang *et al.*, 2011). Expression level of *Osh36* and *RCCR1* were up-regulated in *es2* at 1, and 3 days and 1 day after dark incubation, respectively (Fig. 4c and d).

SAGs expression were activated in *es2*: SAGs were assessed in our study to monitor chlorophyll degradation process. *SGR* is necessary for chlorophyll breakdown, in which leaf senescence enhanced its expression. (Jiang *et al.*, 2007; Hortensteiner, 2009) *Osl85* encodes isocitrate lyase, and was stimulated by senescence in rice (Lee *et al.*, 2001; Fukao *et al.*, 2012), *OsLOX8* was indirectly controlled leaf senescence via jasmonic acid (JA) pathway (Peng *et al.*, 1994; Kong *et al.*, 2006). *HEMA1* a photosynthesis associated gene, encoding NADPH dependent glutamyl-tRNA reductase is an essential enzyme for chlorophyll biosynthetic (Lu *et al.*, 2017; Su *et al.*, 2017). In this study, we conducted qRT-PCR to determine SAGs expression level between WT and *es2*. The result showed that *SGR*, *Osl85*, and *OsLOX8* expression levels were significantly up-regulated in *es2* (Fig. 5a, b, and c, respectively), indicating that accelerated breakdown of chlorophyll and enhanced senescence occurred in *es2*. Meanwhile, *HEMA1* was significantly down-regulated in *es2* suggesting that chlorophyll biosynthesis, particularly, photosynthesis pathway has been disrupted in *es2* (Fig. 5d).

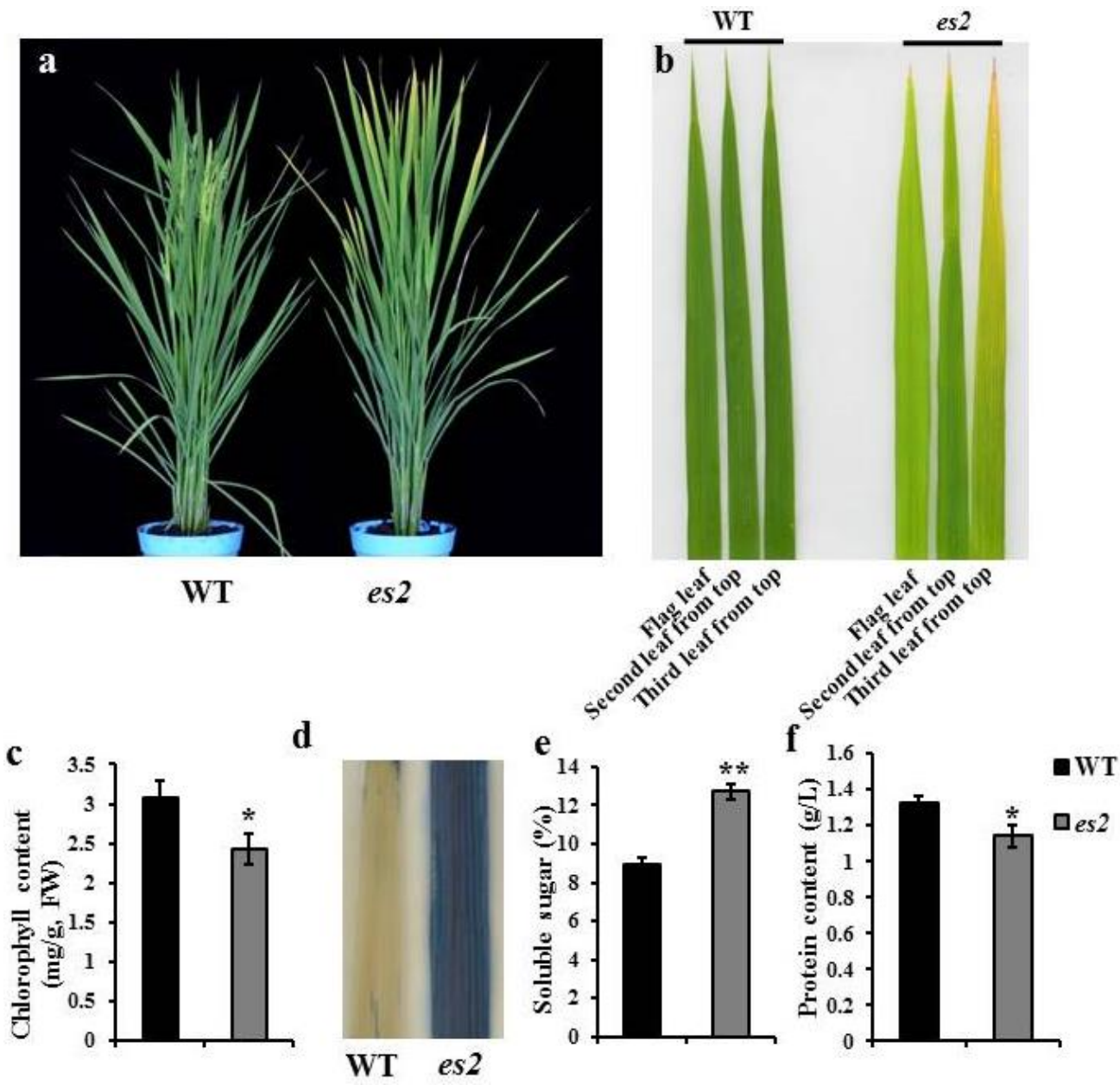

Fig. 1. Morphology comparison of the WT and *es2* at ~75 days after sowing. (a) Whole plant, (b) Three upper leaves, (c) Chlorophyll content from the second leaf from top, (d) Evans blue assay from the second leaf from top, (e) Percentage of soluble sugar, and (f) Protein content. Data shown are means ± SD of three biological replicates; *P* value is determined by the Student's *t* test; *$p \leq 0.05$, **$p \leq 0.01$.

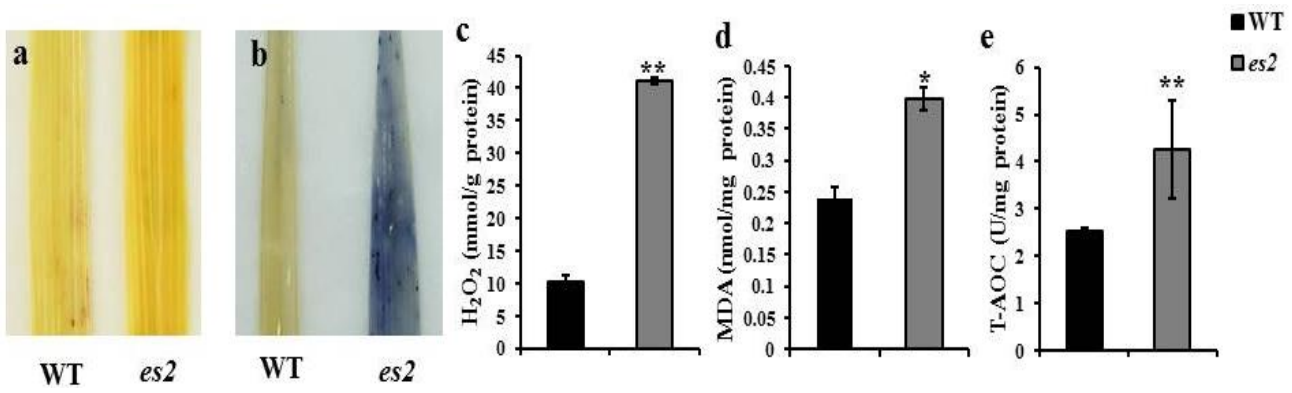

Fig. 2. Reactive oxygen species (ROS) assessment. (a) DAB staining, (b) NBT staining, (c) H_2O_2 content, (d) MDA content, (e) T-AOC content. Data shown are mean ± SD of three biological replicates; *P* value is determined by the Student's *t* test; *$p \leq 0.05$; **$p \leq 0.01$.

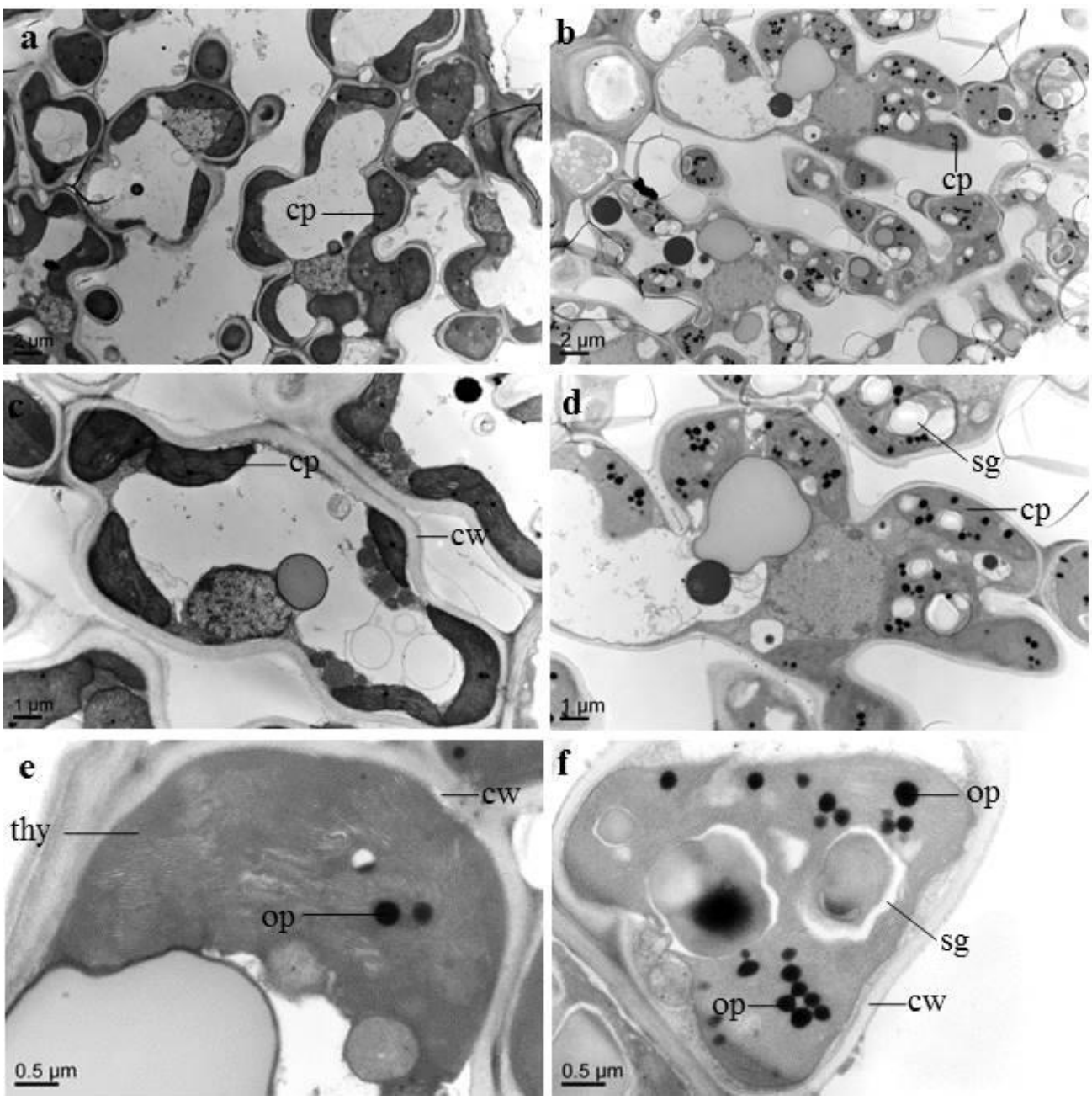

Fig. 3. Ultrastructure of chloroplast at mesophyll layer from the second leaf from top of WT and *es2* using TEM. (a, c, e) WT chloroplast ultrastructure. (b, d, f) *es2* chloroplast ultrastructure. cp, chloroplast; cw, cell wall; thy, thylakoid; op, osmiophilic plastoglobuli; sg, starch granule.

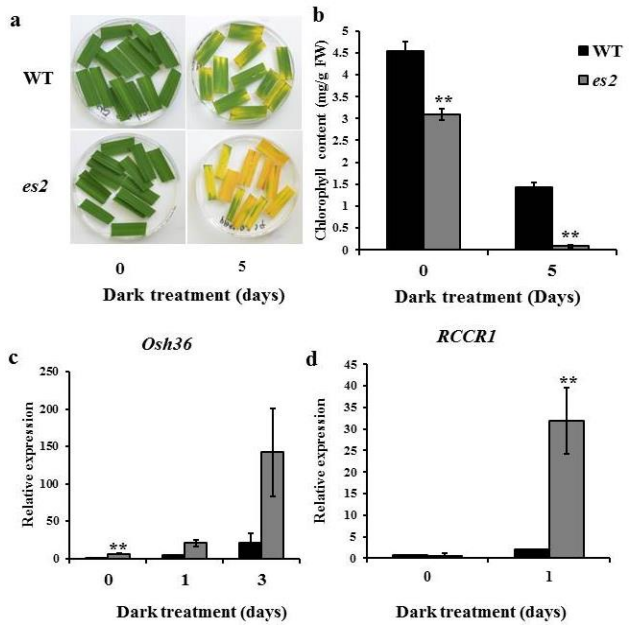

Fig. 4. Morphological appearance and molecular marker of wild type and *es2* before and after dark induced senescence. (a) Detached leaf of WT and *es2* before and after 5 days under dark-incubation, (b) Chlorophyll content of detached leaf showed in Fig. 4a, (c) *Osh36* expression level at 0, 1 and 3 days under dark incubation, and (d) *RCCR1* expression level at 0 and 1 days under dark incubation. Data shown are mean ± SD of three biological replicates; *P* value is determined by the Student's *t* test; $^{**}p \leq 0.01$.

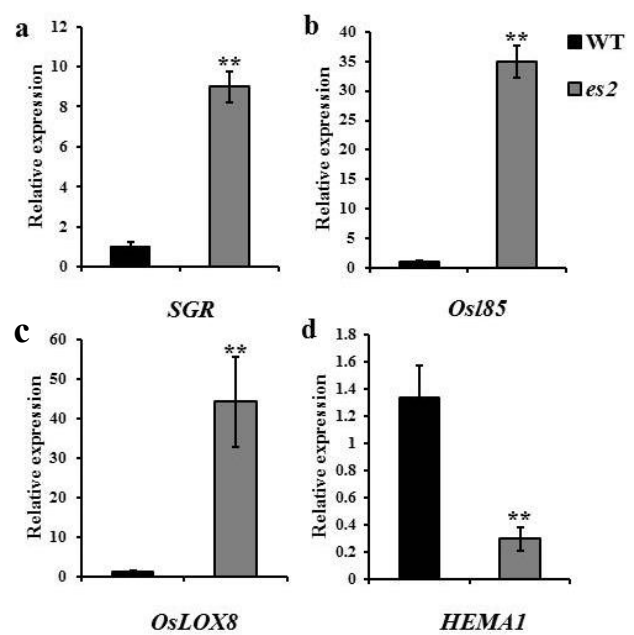

Fig. 5. Transcription level of some SAGs in wild type and *es2*. (a) *SGR*, (b) *Osl85*, (c) *OsLOX8*, (d) *HEMA1*. Data shown are means ± SD of three biological replicates; *P* value is determined by the Student's *t* test; $^{**}p \leq 0.01$.

Decreased NPR in *es2* results in yield loses: Previous report demonstrated that leaf senescence reduce photosynthetic rate (Thomas, 2013), in which affect yield. In present study, we assessed the net photosynthetic rate (NPR) of flag leaves of the WT and *es2* for 5 weeks, beginning at the heading period. The results showed that NPR of *es2* was significantly decreased, compare to the WT, at all the time since heading period onward (Fig. 6a). Further, we found that NPR of *es2* was in the similar pattern as in WT during first two weeks, but sharply decreased during 14-28 days after heading stage (Fig. 6a). It should be noted that lowering of NPR was in correspondence with lower chlorophyll content from flag leaves in *es2* (Fig. 6b). Further, we investigated NPR of flag leaf, the second leaf, and the third leaf from top at the heading period. The result indicated that NPR at the heading period of *es2* was lower than in the WT of all three upper leaves (Fig. 6c).

To determine whether important agronomic traits in *es2* were affected by decreased NPR, we investigated several important agronomic traits in the WT and *es2*. Expectedly, the grain size of *es2* was smaller than that of WT (Fig. 7a), similarly, both 1000-grain weight and the number of grains per panicle were also significantly reduced in *es2* (Fig. 7b and c). However, it should be noted that the panicle length was unaffected in *es2* (Fig. 7d and e), and the seed setting rate of *es2* had no obvious difference (Fig. 7f).

Preliminary mapping of *es2*: F_1 plant derived from *es2* and Zh8015 cross exhibited normal leaf phenotype. In F_2 population, the ratio of normal phenotype: early senescence was ~3:1 ($\chi^2_{3:1, \alpha=0.05, df=1}$, calculate = 0.24, $<\chi^2_{3:1}$ table= 3.84,), suggested that *es2* was regulated by a recessive nuclear gene. Preliminary mapping of *es2* was performed using the golden section strategy, based on the theory that a closer genetic distance corresponds to a closer of physical distance (Chi *et al.*, 2008). As a result, a candidate region was delimited between RM12538 and RM12729 with 2.8 Mb distance (Fig. 8).

Discussion

Leaf senescence is the final stage of leaf development. It is regulated by various genes and associated with enormous internal and external factors. In present study, we identified early leaf senescence, termed *es2*. Here, the physiological appearance, senescence characteristics, and mapping of *es2* were characterized and interrogated. Internal soluble sugar content is one of important leaf senescence marker. Elevation of soluble sugar content reduces NPR and promotes leaf senescence (Lim *et al.*, 2007; Shi *et al.*, 2016). In *es2*, yellowish leaf was accompanied by higher cell death, higher sugar content, and lower NPR level compared to WT. These factors probably contain cross-talk signal and favor each other to promote leaf senescence in *es2*. Up-regulation of SAGs, another senescence marker, is occurred to facilitate chlorophyll degradation and nutrients remobilization. In *es2*, SAGs such as chlorophyll breakdown gene, *SGR*, and two senescence stimulating genes, *Osl85*, and *OsLOX8*, were up-regulated. Elevation of the expression level of these marker genes in *es2* might play an important role in control other factors and, therefore, induce senescence widespread. Up-regulation of these genes are in consistent with a number of previous leaf senescence mutant reports (Kong *et al.*, 2006; Fukao *et al.*, 2012; Liang *et al.*, 2014). Molecular evidence together with histochemical staining, chloroplast structure and a number of leaf senescence physiology aspects are according to expected results from leaf senescence mutant. Further question is mutant of *es2* caused less chlorophyll synthesis than usual or enhanced chlorophyll degradation process?

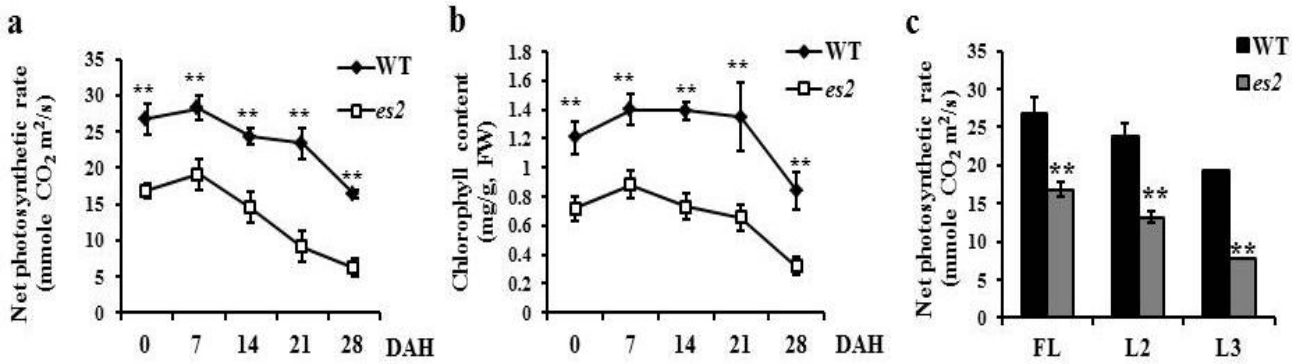

Fig. 6. Correspondence of net photosynthetic rate (NPR) and chlorophyll content of wild type and *es2*. (a) NPR from flag leaf every 7 days for 5 weeks beginning at heading date period, (b) Chlorophyll content from flag leaves every 7 days for 5 weeks beginning at heading date period, and (c) NPR of WT and *es2* in FL, L2, and L3. FL, flag leaf, L2, the second leaf from top, L3, the third leaf from top at heading period. Data shown are mean ± SD of three biological replicates. *P* value is determined by the Student's *t* test; $^{**}p \leq 0.01$ DAH, days after heading.

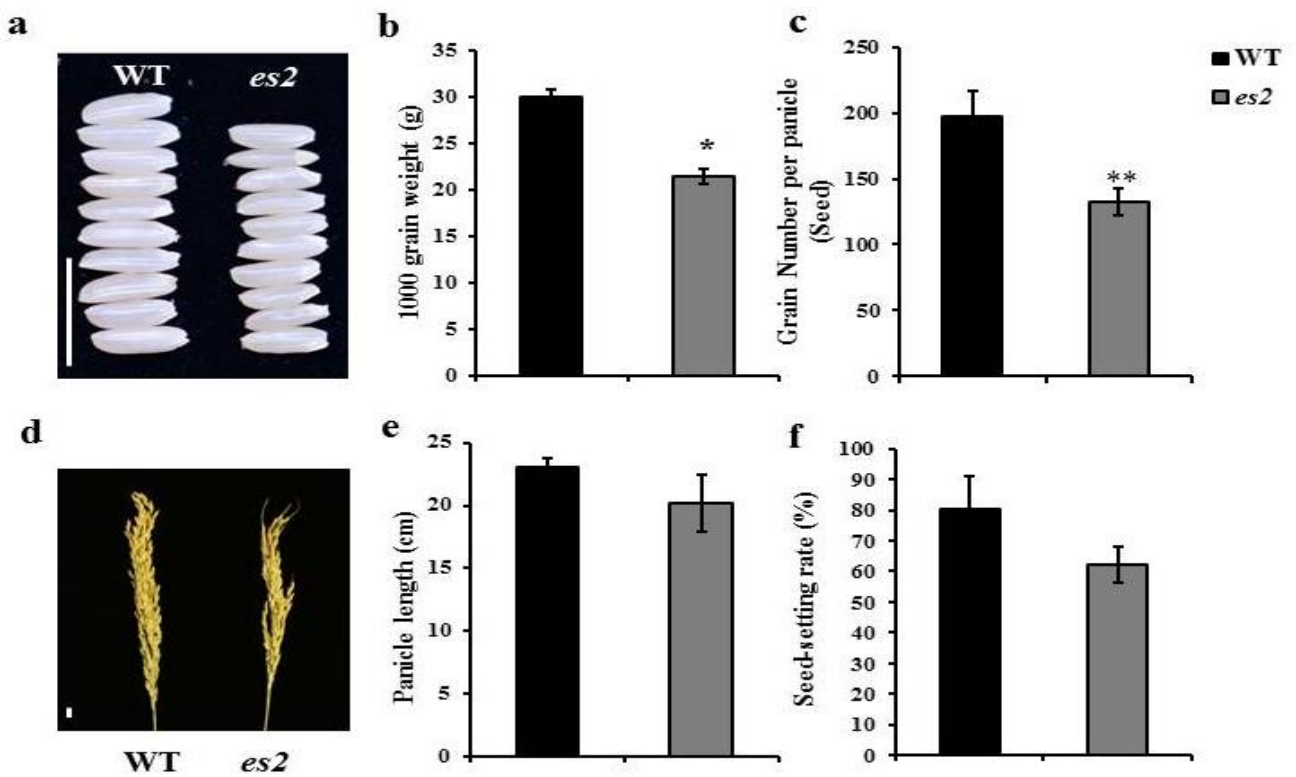

Fig. 7. Yield-related agronomic traits of the wild type and *es2* related to yield. (a) Grain size, (b) 1000 grain weight, (c) Grain number per panicle, (d) Panicle morphology, (e) Panicle length, and (f) Percentage of seed-setting rate. Data shown are mean ± SD of five biological replicates. *P* value is determined by the Student's *t* test $^{*}p \leq 0.05$; $^{**}p \leq 0.01$, Bars = 1 cm.

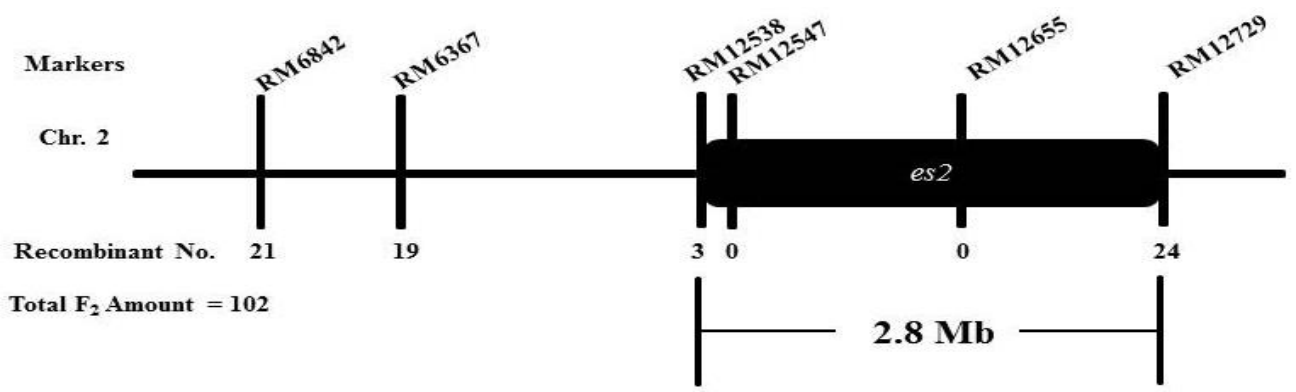

Fig. 8. Preliminary mapping result of *es2* on chromosome 2. Physical mapping was identified by RM12538 and RM12729 markers on the short arm of chromosome 2.

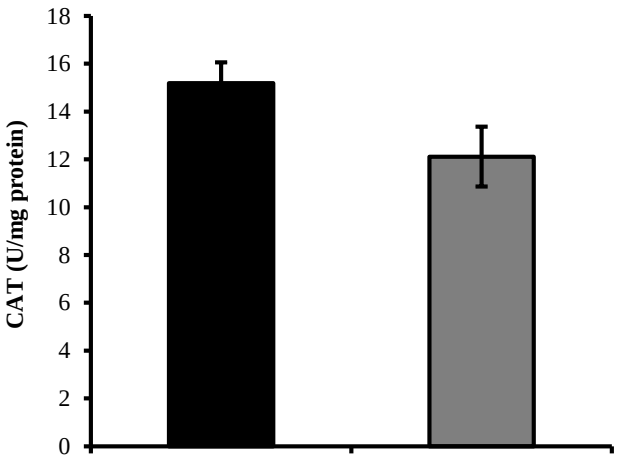

Supplemental Fig. 1. ROS enzymatic marker. Catalase (CAT) activity in WT and *es2*.

In order to determine oxidative stress and byproducts level to investigate whether these factors are presented in *es2*, oxidative stress such as ROS and its byproducts level were determined in WT and *es2*. NBT and DAB assay indicated that superoxide and H_2O_2, respectively, were cumulated in *es2* at higher level. Histochemical staining assay have previously been reported correspondingly and are proved similar in a number of leaf senescence studies (Li *et al.*, 2014; Deng *et al.*, 2017; Mao *et al.*, 2017). Supporting with histochemical assay result, H_2O_2 and MDA content were increased in *es2*, while protein content and was decreased. The results suggested that peroxidation occurred, as a result, oxidative stress increase in *es2* and probably cause lowering of CAT level. Higher MDA content found in *es2* is likely because of higher cell phospholipid has damaged by ROS oxidation reaction (Del Rio *et al*., 2005; Bi *et al.*, 2017), therefore, oxidative stress was higher in *es2*. These results suggest that ROS has accumulated in *es2* and induces signal transduction cascade and, finally, resulted in leaf senescence. In our study, T-AOC activity was increased in *es2*, of which unconventional in leaf senescence mutant. It is possible that higher oxidative stress caused *es2* evolve higher T-AOC activity. In addition, as in many other leaf senescence mutant studies (Li *et al.*, 2014; Deng *et al.*, 2017), irregular chloroplast ultrastructure was found in *es2*. Large size of starch granules and high amount of plastoglobuli in *es2* indicated that plant enters leaf senescence. Moreover, we speculated that larger size of starch granules take over grana formation area, and probably caused energy shortage in *es2*. Starch hyper-accumulation is the common symptom across leaf senescence studies (Li *et al.*, 2014; He *et al.*, 2018). We hypothesized that deficient of energy due to lowering of NPR and chlorophyll content might serially cause poor grain filling. In our study, agronomic traits such as grain size, 1000-grain weight, and grain number per panicle were reduced in *es2*. Further, all these detected physiologies are consistent in other previous leaf senescence studies (Wu *et al.*, 2013; Li *et al.*, 2014; Deng *et al.*, 2017). Therefore, we suggest that *es2* was true leaf senescence mutant.

Majority causes of leaf senescence are belonged to chlorophyll biosynthesis block and/or enhanced of chlorophyll degradation process. A large number of chlorophyll biosynthesis mutant have previously been reported. For instance, *sdl*, exerts white leaf color during seedling stage. The elder leaf could slowly recover into strip green after younger leaf exert thereafter (Qin *et al.*, 2017). *al1* exhibits albino since germination and died after three leaves stage (Zhao *et al.*, 2016). *swl1* exhibits variegated albino seedlings and could not grow beyond seedling stage (Hayashi-Tsugane *et al.*, 2014). While enhanced chlorophyll degradation mutant usually exhibited yellow leaf during tillering stage. *gogat1*, *yld1*, *mps1* exhibit normal leaf at seedling stage but leaf turned yellow during tillering stage (Liu *et al.*, 2016; Deng *et al.*, 2017; Zeng *et al.*, 2017), suggesting that chlorophyll biosynthesis mutants usually exhibit normal leaf during seedling stage, however, deficiency caused by mutate gene lead to senescence during tillering stage afterward. In present study, *es2* exhibited yellow leaf at late tillering stage, suggesting that *es2* likely fell into enhanced chlorophyll degradation category. Higher *SGR* expression level and dark induced senescence evidenced that *es2* contained stimulated chlorophyll degradation activity. The mutate gene of *es2* might function as an inhibitor of chlorophyll degrading factors or probably transcription factor that negatively regulated chlorophyll degrading genes.

Defect of chlorophyll maintenance caused by mutation of the corresponding gene alters leaf photosynthetic ability is likely caused senescence in *es*2. Previous studies indicated that leaf senescence related function genes have been cloned and characterized. *OsFd*‑*GOGAT* is likely required for nitrogen recycling process in rice (Zeng *et al.*, 2017). *SGR* induces chlorophyll breakdown reaction (Jiang *et al.*, 2007). *OsSWEET5* is regulates the cross-talk of auxin and sugar level (Zhou *et al.*, 2014). Two NAC transcription factors, *OsNAC2* and *OsNAP*, promote leaf senescence and both are induced by ABA (Liang *et al.*, 2014; Mao *et al.*, 2017). To our angle, although a number of senescence-related genes have been identified, however, because leaf senescence is the complex phenomena and many genes participate, therefore, novel mutant offers a crucial opportunity to understand, in some case, new leaf senescence regulatory network. In our study, *es2* treated by EMS exhibited early senescence at late tillering stage offer an opportunity to investigate novel senescence mutant. A number of evidences favoring leaf senescence were uncovered and proved in *es2*, suggesting that *es2* was genuine senescence mutant and, therefore, useful for senescence study in rice. Genetic analysis clearly demonstrated that recessive nuclear mutant gene caused senescence in *es2*. Ultimately, *es2* was mapped on the short arm of chromosome2 between RM12538 and RM12729. Further study will be conducted to narrow down the region in order to identify senescence responsible gene in *es2*. Further study could address precise gene location and in-depth study of leaf senescence.

Acknowledgments

This work is supported by the National Key Transform Program (#2016ZX08001-002), the National Natural Science Foundation of China (#31501290), the Zhejiang Provincial Natural Science Foundation of China (Grant #LQ14C130003), the Super Rice Breeding Innovation Team and Rice Heterosis Mechanism Research Innovation Team of the Chinese Academy of Agricultural Sciences Innovation Project (CAAS-ASTIP-2013-CNRRI) and the National Natural Science Foundation of China (NSFC 31521064).

References

Bi, Z., Y. Zhang, W. Wu, X. Zhan, N. Yu, T. Xu, Q. Liu, Z. Li, X. Shen, D. Chen, S. Cheng and L. Cao. 2017. *ES7*, encoding a ferredoxin-dependent glutamate synthase, functions in nitrogen metabolism and impacts leaf senescence in rice. *Plant science*, 259: 24-34.

BuchananWollaston, V. and C. Ainsworth. 1997. Leaf senescence in *Brassica napus*: Cloning of senescence related genes by subtractive hybridisation. *Plant Mol. Biol*., 33(5): 821-834.

Chakrabarty, D., J. Chatterjee and S.K. Datta. 2007. Oxidative stress and antioxidant activity as the basis of senescence in chrysanthemum florets. *Plant Growth Regul*., 53(2): 107-115.

Chelikani, P., I. Fita and P.C. Loewen. 2004. Diversity of structures and properties among catalases. *Cell Mol. Life Sci*., 61(2): 192-208.

Chi, X.F., X.Y. Lou and Q.Y. Shu. 2008. Progressive fine mapping in experimental populations: An improved strategy toward positional cloning. *J. Theor. Biol*., 253(4): 817-823.

Del Rio, D., A.J. Stewart and N. Pellegrini. 2005. A review of recent studies on malondialdehyde as toxic molecule and biological marker of oxidative stress. *Nutr. Metab. Cardiovas*., 15(4): 316-328.

Deng, L.C., P. Qin, Z. Liu, G.L. Wang, W.L. Chen, J.H. Tong, L.T. Xiao, B. Tu, Y.T. Sun, W. Yan, H. He, J. Tan, X.W. Chen, Y.P. Wang, S.G. Li and B.T. Ma. 2017. Characterization and fine-mapping of a novel premature leaf senescence mutant *yellow leaf and dwarf 1* in rice. *Plant Physiol. Bioch*., 111: 50-58.

Fukao, T., E. Yeung and J. Bailey-Serres. 2012. The submergence tolerance gene *SUB1A* delays leaf senescence under prolonged darkness through hormonal regulation in rice. *Plant Physiol*., 160(4): 1795-1807.

Gan, S., 2007. Senescence processes in plants. *Oxford, UK: Blackwell Publishing*: 145-170.

Guo, Y., Z. Cai and S. Gan. 2004. Transcriptome of *Arabidopsis* leaf senescence. *Plant Cell and Environment*, 27(5): 521-549.

Guo, Y.F. and S.S. Gan. 2005. Leaf senescence: Signals, execution, and regulation. *Curr. Top. Dev. Biol*., 71: 83-112.

Hayashi-Tsugane, M., H. Takahara, N. Ahmed, E. Himi, K. Takagi, S. Iida, K. Tsugane and M. Maekawa. 2014. A mutable albino allele in rice reveals that formation of thylakoid membranes requires the *SNOW-WHITE LEAF1* gene. *Plant Cell Physiol*., 55(1): 3-15.

He Y., L.J. Li, Z.H. Zhang and J.L. Wu. 2018. Identification and comparative analysis of premature senescence leaf mutants in rice (*Oryza sativa* L.). *Int. J. Mol. Sci*., 19(140).

Hortensteiner, S. 2009. Stay-green regulates chlorophyll and chlorophyll-binding protein degradation during senescence. *Trends in plant science*, 14(3): 155-162.

Jan, A., K. Maruyama, D. Todaka, S. Kidokoro, M. Abo, E. Yoshimura, K. Shinozaki, K. Nakashima and K. Yamaguchi-Shinozaki. 2013. OsTZF1, a ccch-tandem zinc finger protein, confers delayed senescence and stress tolerance in rice by regulating stress-related genes. *Plant Physiol*., 161(3): 1202-1216.

Jiang, H.W., M.R. Li, N.B. Liang, H.B. Yan, Y.L. Wei, X. Xu, J.F. Liu, Z. Xu, F. Chen and G.J. Wu. 2007. Molecular cloning and function analysis of the *stay green* gene in rice. *Plant J*., 52(2): 197-209.

Jongebloed, U., J. Szederkenyi, K. Hartig, C. Schobert and E. Komor. 2004. Sequence of morphological and physiological events during natural ageing and senescence of a castor bean leaf: Sieve tube occlusion and carbohydrate back-up precede chlorophyll degradation. *Physiol. Plant*, 120(2): 338-346.

Kong, X.P. and D.Q. Li. 2011. Hydrogen peroxide is not involved in hrpn from *Erwinia amylovora*-induced hypersensitive cell death in maize leaves. *Plant Cell Rep*., 30(7): 1273-1279.

Kong, Z.S., M.N. Li, W.Q. Yang, W.Y. Xu and Y.B. Xue. 2006. A novel nuclear-localized CCCH-type zinc finger protein, OsDOS, is involved in delaying leaf senescence in rice. *Plant Physiol*., 141(4): 1376-1388.

Lee, R.H., C.H. Wang, L.T. Huang and S.C.G. Chen. 2001. Leaf senescence in rice plants: Cloning and characterization of senescence up-regulated genes. *J. Exp. Bot*., 52(358): 1117-1121.

Leng, Y.J., Y.L. Yang, D.Y. Ren, L.C. Huang, L.P. Dai, Y.Q. Wang, L. Chen, Z.J. Tu, Y.H. Gao, X.Y. Li, L. Zhu, J. Hu, G.H. Zhang, Z.Y. Gao, L.B. Guo, Z.S. Kong, Y.J. Lin, Q. Qian and D.L. Zeng. 2017. A rice *PECTATE LYASE-LIKE* gene is required for plant growth and leaf senescence. *Plant Physiol*., 174(2): 1151-1166.

Li, Z., Y.X. Zhang, L. Liu, Q.E. Liu, Z.Z. Bi, N. Yu, S.H. Cheng and L.Y. Cao. 2014. Fine mapping of the lesion mimic and early senescence 1 (*lmes1*) in rice (*Oryza sativa*). *Plant Physiol. Bioch*., 80: 300-307.

Liang, C., Y. Wang, Y. Zhu, J. Tang, B. Hu, L. Liu, S. Ou, H. Wu, X. Sun, J. Chu and C. Chu. 2014. OsNAP connects abscisic acid and leaf senescence by fine-tuning abscisic acid biosynthesis and directly targeting senescence-associated genes in rice. *Proc. Natl. Acad. Sci. USA*, 111(27): 10013-10018.

Lim, P.O., H.J. Kim and H.G. Nam. 2007. Leaf senescence. *Annu. Rev. Plant Biol*., 58: 115-136.

Liu, Z.X., Y. Cui, Z.W. Wang, Y.H. Xie, X.C. Sang, Z.L. Yang, C.W. Zhang, F.M. Zhao, G.H. He and Y.H. Ling. 2016. Phenotypic characterization and fine mapping of *mps1*, a premature leaf senescence mutant in rice (*Oryza sativa* L.). *J. Integr. Agr*., 15(9): 1944-1954.

Lu, G., J.A. Casaretto, S. Ying, K. Mahmood, F. Liu, Y.M. Bi and S.J. Rothstein. 2017. Overexpression of *OsGATA12* regulates chlorophyll content, delays plant senescence and improves rice yield under high density planting. *Plant Mol. Biol*., 94(1-2): 215-227.

Mao, C., S. Lu, B. Lv, B. Zhang, J. Shen, J. He, L. Luo, D. Xi, X. Chen and F. Ming. 2017. A rice NAC transcription factor promotes leaf senescence via aba biosynthesis. *Plant physiol*., 174(3): 1747-1763.

McCouch, S.R., L. Teytelman, Y. Xu, K.B. Lobos, K. Clare, M. Walton, B. Fu, R. Maghirang, Z. Li, Y. Xing, Q. Zhang, I. Kono, M. Yano, R. Fjellstrom, G. DeClerck, D. Schneider, S. Cartinhour, D. Ware and L. Stein. 2002. Development and mapping of 2240 new SSR markers for rice (*Oryza sativa* L.). *DNA research*, 9(6): 199-207.

Murray, M.G. and W.F. Thompson. 1980. Rapid isolation of high molecular weight plant DNA. *Nucleic acids research*, 8(19): 4321-4325.

Nam, H.G. 1997. The molecular genetic analysis of leaf senescence. *Curr. Opin. Biotech*., 8(2): 200-207.

Navabpour, S., K. Morris, R. Allen, E. Harrison, S. A-H-Mackerness and V. Buchanan-Wollaston. 2003. Expression of senescence-enhanced genes in response to oxidative stress. *J. Exp. Bot*., 54(391): 2285-2292.

Nooden, L.D., J.J. Guiamet and I. John. 1997. Senescence mechanisms. *Physiol Plantarum*, 101(4): 746-753.

Peng, Y.L., Y. Shirano, H. Ohta, T. Hibino, K. Tanaka and D. Shibata. 1994. A novel lipoxygenase from rice. Primary structure and specific expression upon incompatible infection with rice blast fungus. *The Journal of Biological Chemistry*, 269(5): 3755-3761.

Qin, R., D. Zeng, R. Liang, C. Yang, D. Akhter, M. Alamin, X. Jin and C. Shi. 2017. Rice gene *SDL/RNRS1*, encoding the small subunit of ribonucleotide reductase, is required for chlorophyll synthesis and plant growth development. *Gene*, 627: 351-362.

Quirino, B.F., Y.S. Noh, E. Himelblau and R.M. Amasino. 2000. Molecular aspects of leaf senescence. *Trends in Plant Science*, 5(7): 278-282.

Quirino, B.F., W.D. Reiter and R.D. Amasino. 2001. One of two tandem Arabidopsis genes homologous to monosaccharide transporters is senescence-associated. *Plant Mol. Biol*., 46(4): 447-457.

Ricachenevsky, F.K., R.A. Sperotto, P.K. Menguer and J.P. Fett. 2010. Identification of Fe-excess-induced genes in rice shoots reveals a WRKY transcription factor responsive to Fe, drought and senescence. *Molecular Biology Reports*, 37(8): 3735-3745.

Shi, H., B. Wang, P. Yang, Y. Li and F. Miao. 2016. Differences in sugar accumulation and mobilization between sequential and non-sequential senescence wheat cultivars under natural and drought conditions. *PloS one*, 11(11): e0166155.

Su, Y., S.K. Hu, B. Zhang, W.J. Ye, Y.F. Niu, L.B. Guo and Q. Qian. 2017. Characterization and fine mapping of a new early leaf senescence mutant *es3(t)* in rice. *Plant Growth Regul*, 81(3): 419-431.

Tang, Y.Y., M.R. Li, Y.P. Chen, P.Z. Wu, G.J. Wu and H.W. Jiang. 2011. Knockdown of *OsPAO* and *OsRCCR1* cause different plant death phenotypes in rice. *J. Plant Physiol*., 168(16): 1952-1959.

Thomas, H. 2013. Senescence, ageing and death of the whole plant. *New Phytologist*, 197(3): 696-711.

ThordalChristensen, H., Z.G. Zhang, Y.D. Wei and D.B. Collinge. 1997. Subcellular localization of H_2O_2 in plants. H_2O_2 accumulation in papillae and hypersensitive response during the barley-powdery mildew interaction. *Plant J*., 11(6): 1187-1194.

van Doorn, W.G. and E.J. Woltering. 2004. Senescence and programmed cell death: Substance or semantics? *J. Exp. Bot*., 55(406): 2147-2153.

Wang, Y.Q., A.H. Lin, G.J. Loake and C.C. Chu. 2013. H_2O_2-induced leaf cell death and the crosstalk of reactive nitric/oxygen species. *J Integr. Plant Biol*., 55(3): 202-208.

Wingler, A., A. von Schaewen, R.C. Leegood, P.J. Lea and W.P. Quick. 1998. Regulation of leaf senescence by cytokinin, sugars, and light - effects on NADH-dependent hydroxypyruvate reductase. *Plant Physiol*., 116(1): 329-335.

Woo, H.R., H.J. Kim, H.G. Nam and P.O. Lim. 2013. Plant leaf senescence and death - regulation by multiple layers of control and implications for aging in general. *J. Cell Sci*., 126(21): 4823-4833.

Wu, H.B., B. Wang, Y.L. Chen, Y.G. Liu and L.T. Chen. 2013. Characterization and fine mapping of the rice premature senescence mutant *ospse1*. *Theor. Appl. Genet*., 126(7): 1897-1907.

Zeng, D.D., R. Qin, M. Li, M. Alamin, X.L. Jin, Y. Liu and C.H. Shi. 2017. The ferredoxin-dependent glutamate synthase (OsFd-GOGAT) participates in leaf senescence and the nitrogen remobilization in rice. *Mol. Genet. Genomics*, 292(2): 385-395.

Zhao, D.S., C.Q. Zhang, Q.F. Li, Q.Q. Yang, M.H. Gu and Q.Q. Liu. 2016. A residue substitution in the plastid ribosomal protein L12/AL1 produces defective plastid ribosome and causes early seedling lethality in rice. *Plant Mol. Biol*., 91(1-2): 161-177.

Zhou, Y., L. Liu, W.F. Huang, M. Yuan, F. Zhou, X.H. Li and Y.J. Lin. 2014. Overexpression of *OsSWEET5* in rice causes growth retardation and precocious senescence. *PloS one*, 9(4): e94210.

(Received for publication 28 November 2018)